Subband Signal Separation

Jörgen Nordberg[1], Hai Huyen Dam[2] and Sven Nordholm[3]

[2] Blekinge Institute of Technology, 372 25 Sweden. E-mail: Jorgen.Nordberg@bth.se.

[2]Australian Telecommunications Research Institute, Curtin University of Technology, Perth, Australia and Australian Telecommunications CRC. E-mail: dam@atri.curtin.edu.au.

[3] Australian Telecommunications Research Institute, Curtin University of Technology, Perth, Australia and Australian Telecommunications CRC. E-mail: sven@atri.curtin.edu.au.

Abstract

In wireless communication, the transmitted signals arrive at the receiver will be subjected to multipath propagation, i.e. the signals will be received with different time delays and attenuations. It is therefore not enough to use only a spatial receiver since such a receiver can not exploit the multipath properties. A temporal receiver, on the other hand, works well for multipath situations but does not utilize the spatial information which is of vital importance in multiuser systems. Thus, a combined spatial and temporal receiver structure can utilize multipath, spatial distribution and independence properties of the multiple sources. Such a spatial-temporal receiver structure is usually computationally complex. In this paper a subband signals separator is presented to reduce the required complexity without a significantly reduction in performance. The subband signal separator will be compared with its fullband equivalent using performance measures as the complexity and mean-square-error. Simulation results show that up to 82 % reduction in the computationally complexity with only a slightly degradation in mean square error performance.

1 Introduction

The demand of increasing capacity in future and existing wireless communication systems have recently resulted in a lot of interest into smart antennas and multi-input multi-output (MIMO) systems [1]. For MIMO systems, the multipath richness of the channel where several versions of the transmitted signals arrive at the receiver with different delays and attenuations determines the channel capacity. It is not enough to use only a spatial receiver since such a receiver can not exploit the multipath properties. A temporal receiver structure, on the other hand, works well for multipath situations but does not utilize the spatial information which is of vital importance in multiuser systems. Thus, a combined spatial and temporal receiver structure will provide a solution to these demands.

The transmitted signals are mixed in the channel by multi-paths having different attenuations and delays. The receiver takes the signals at each antenna element and un-mixes them as close as possible to the original transmitted signals. The spatial-temporal receiver can utilize multipath, spatial diversity and independence properties of the multiple sources. One of the major concerns in using this type of receiver is the complexity. The computational cost can be substantially reduced by using a multi-rate signal processing receiver.

The multi-rate signal processing technique employed here is a delayless filterbank (FB) procedure [2]. This technique uses the advantage of multi-rate signal processing for the implementation of the algorithm but avoids the filterbank and block processing delays by transforming the un-mixing subband filters to an un-mixing fullband filter. The difference in signal separation performance of subband and fullband solution depends on the filterbank and the subband to fullband transformation.

The delayless signal separation has been investigated in [3]. In this paper, a filter bank design method is considered to improve signal separation performance. This performance depends on both the in-band aliasing and design of the filterbank for a fixed cut-off frequency. Both the in-band aliasing and the filter performance with respect to the least square criterion can be formulated as quadratic functions of the filter coefficients. The design problem becomes to minimize filter performance with respect to some acceptable attenuation in the passband. This problem can be formulated as a semi-infinite quadratic programming problem, which can be solved using recently developed semi-infinite quadratic programming approach

[4] or conventional discretization approach.

Simulation results show that the delayless multirate implementation has approximately the same separation performance as the fullband but with a few percentage of the computational complexity. The computational complexity for the subband and the fullband scheme is compared by using a relative number of floating point operations (RFLOPS) measure. This RFLOPS is based on the number of the fullband floating point operation (FLOPS). The RFLOPS is reduced when the number of subband increases at the expense of the separation performance. The trade-off in performance of the mean square error (MSE) and the RFLOPS for different number of subbands is also discussed.

2 System Model

Consider the system model given in Figure 1. The statistically independent source bits are generated with equal probabilities and modulated using binary phase shift keying (BPSK).

The S transmitting signals are denoted as

$$\mathbf{s}[n] = [s_1[n], \cdots, s_S[n]],$$

where n is the time index through a medium, i.e. air, water or space. At the receiver, an array of I sensors picks up a set of signals

$$\mathbf{x}[n] = [x_1[n], \cdots, x_I[n]],$$

where $x_i[n]$, $1 \leq i \leq I$, is the received signal from the channel. The channel represents the medium which affects on the transmitting signals and the transmitting filters and can be described through propagation models consisting of doppler effects. This channel can be modeled as a time varying FIR channel mixing matrix with different characteristics such as deep nulls and multipath propagation. Denote the mixing matrix $\mathbf{C}$ as

$$\mathbf{C} = \begin{bmatrix} \mathbf{c}_{11} & \cdots & \mathbf{c}_{1S} \\ \vdots & \ddots & \vdots \\ \mathbf{c}_{I1} & \cdots & \mathbf{c}_{IS} \end{bmatrix} \tag{1}$$

where

$$\mathbf{c}_{ik} = [c_{ik}[0], \cdots, c_{ik}[N-1]]^T, 1 \leq i \leq I \text{ and } 1 \leq k \leq S$$

is the channel impulse response of length N from the k^{th} transmitted signal to the i^{th} sensor.

The received signal at the i^{th} sensor, $1 \leq i \leq I$, in a noise free case is given as

$$x_i[n] = \sum_{k=1}^{S} \sum_{l=0}^{N-1} c_{ik}[l] s_k[n-l]. \tag{2}$$

The signal $x_i[n]$ is then presented to un-mixing filters. These un-mixing filters estimates the inverse of the channel mixing filters which can have non-minimum or minimum phase response. If the channel mixing filters have non-minimum phase response, i.e. some of their zeros are outside the unit circle, their true inverting causal filters are not bounded. However, there exit bounded non-causal inverse filters. A delay τ_D is included in the receiver to enable a finite length approximation of the inverting filters, see Figure 2. Denote

$$\mathbf{w}_{ik} = [w_{ik}[0], \cdots, w_{ik}[L-1]]^T$$

as the impulse response of the un-mixing filter from the sensor signal $x_i[n]$ to the output $u_k[n]$. The filter length L is chosen so that the transmitted signal $s_k[n]$ can be recovered. The un-mixing filters form the following un-mixing matrix

$$\mathbf{W} = \begin{bmatrix} \mathbf{w}_{11} & \cdots & \mathbf{w}_{1S} \\ \vdots & \ddots & \vdots \\ \mathbf{w}_{I1} & \cdots & \mathbf{w}_{IS} \end{bmatrix}. \tag{3}$$

In this study, the number of transmitted signals S is assumed to be equal to the number of sensors with $S = I = 2$. However, the problem can easily be extended for general situations.

In order to study the performance of the delayless subband signal separation method, the source signals are assumed to be known. The optimum un-mixing filters $\mathbf{W}$ is obtained by using the Wiener correlation method. Denote $\mathbf{R}_{x_i,x_k}$ as an $L \times L$ correlation matrix between the sensor signals $x_i[n]$ and $x_k[n]$ and $\mathbf{r}_{x_i,s_k}$ as an $L \times 1$ cross-correlation vector between the sensor signal $x_i[n]$ and the transmitted signal $s_k[n]$. These correlations are estimated from the data by using ensemble average [5]. The impulse response for the un-mixing filters are obtained by solving

$$\mathbf{R}_{\mathbf{xx}} \mathbf{W} = \mathbf{r}_{\mathbf{xs}}, \tag{4}$$

where

$$\mathbf{R}_{\mathbf{xx}} = \begin{bmatrix} \mathbf{R}_{x_1,x_1} & \mathbf{R}_{x_1,x_2} \\ \mathbf{R}_{x_2,x_1} & \mathbf{R}_{x_2,x_2} \end{bmatrix},$$

$$\mathbf{W} = \begin{bmatrix} \mathbf{w}_{11} & \mathbf{w}_{12} \\ \mathbf{w}_{21} & \mathbf{w}_{22} \end{bmatrix},$$

and

$$\mathbf{r}_{\mathbf{xs}} = \begin{bmatrix} \mathbf{r}_{x_1,s_1} & \mathbf{r}_{x_1,s_2} \\ \mathbf{r}_{x_2,s_1} & \mathbf{r}_{x_2,s_2} \end{bmatrix}.$$

These filters also minimize mean squared error between the output signal and the transmitted signal [3]. The output signals from the un-mixing filters are given as follows:

$$u_k[n] = \sum_{i=1}^{2} \sum_{l=0}^{L-1} w_{ik}[l] x_i[n-l], \qquad 1 \leq k \leq 2. \tag{5}$$

3 Delayless Subband Signal Separation

The proposed delayless subband signal separation scheme [2] is presented in Figure 2. The transmitted and the received signals are divided into M frequency bands. The subband un-mixing filters are obtained in each frequency bands by using the optimal Wiener correlation method, see (4). These subband un-mixing filters are transformed into the frequency domain by using a fast Fourier transform (FFT). The frequency response for the fullband un-mixing filters are obtained by stacking different subband frequency responses. The impulse response for the fullband un-mixing filters are the inverse FFT (IFFT) of the stacked fullband frequency response [2].

An uniformly modulated filterbank (UMF) is used to split the signals into different frequency bands. The different subbands filters in the filterbank are the modulated versions of a prototype filter. Thus, the design of the UMF is reduced to the design of a prototype filter with length K and the impulse response $\mathbf{h}$,

$$\mathbf{h} = [h[0], \cdots, h[K-1]]^T \tag{6}$$

where $[.]^T$ denotes the transpose of a vector. The transfer function of the prototype filter becomes

$$H(z) = \sum_{l=0}^{K-1} h[l] z^{-l} = \mathbf{h}^T \phi(z) \tag{7}$$

where $\phi(z) = [1, \cdots, z^{-(K-1)}]^T$.

The transfer function of the m^{th} subband in a UMF is obtained from $H(z)$ as follows

$$H_m(z) = H(zW_M^m) = \sum_{l=0}^{K-1} h[l](zW_M^m)^{-l} \tag{8}$$

where $W_M = e^{-j2\pi/M}$ and $0 \leq m \leq M-1$.

Polyphase decomposition is used to implement the UMF efficiently where the decimation is performed before the subband filtering [6]. To avoid aliasing, the filterbank is oversampled with a factor of two, i.e. the subband signals are decimated by a factor $D = \frac{M}{2}$.

The transformation between subband and fullband depends on the performance of the transfer function $H(z)$ with the corresponding frequency response $H(e^{j\omega})$. In the following section, the design of $H(e^{j\omega})$ will be considered. The desired filter is lowpass with a normalised cut-off frequency $\omega_p = \pi/M$. Since it is desirable to have approximately linear phase in the passband, the desired complex frequency response is specified as

$$H_d(e^{j\omega}) = e^{j\omega\tau}, \qquad \forall \omega \in [-\omega_p, \omega_p] \tag{9}$$

where $\tau = (L-1)/2$.

The most common criteria in filter design are least square and min-max [7]. Since it is important to have a flat passband response for the prototype filter, a least square criterion is chosen in the cost function. However, a min-max criterion is also included in the constraints to restrict the maximum attenuation of the filter within some acceptable region.

The least square and the min-max errors are given as

$$e_1(\mathbf{h}) = \frac{1}{2\omega_p} \int_{-\omega_p}^{\omega_p} |H(e^{j\omega}) - H_d(e^{j\omega})|^2 d\omega \tag{10}$$

and

$$e_2(\mathbf{h}) = \max_{-\omega_p \leq \omega \leq \omega_p} |H(e^{j\omega}) - H_d(e^{j\omega})|. \tag{11}$$

It follows from (7) that $H(e^{j\omega})$ is a linear function of the coefficient $\mathbf{h}$. Thus, (10) is reduced to a quadratic function of $\mathbf{h}$

$$e_1(\mathbf{h}) = \mathbf{h}^T \mathbf{A} \mathbf{h} - 2\mathbf{h}^T \mathbf{b} + 1,$$

where $\mathbf{A}$ is a $K \times K$ matrix

$$\mathbf{A} = \frac{1}{2\omega_p} \int_{-\omega_p}^{\omega_p} \phi(e^{j\omega}) \phi^H(e^{j\omega}) d\omega, \tag{12}$$

and $\mathbf{b}$ is a $K \times 1$ vector

$$\mathbf{b} = \frac{1}{2\omega_p} \int_{-\omega_p}^{\omega_p} \mathcal{R}\{e^{j\omega\tau} \phi^H(e^{j\omega})\} d\omega. \tag{13}$$

The operator $[.]^H$ and $\mathcal{R}\{.\}$ denote the Hermitian operation of a matrix and the real part of a complex function, respectively.

The prototype filter is also designed to have a minimum in-band aliasing effect. Since the transfer functions of the subband filters are related by (8), it is sufficient to minimize the energy in the aliasing terms of the first subband. This aliasing error can be formulated as a quadratic function of $\mathbf{h}$ [8],

$$\beta(\mathbf{h}) = \mathbf{h}^T \mathbf{C} \mathbf{h}, \tag{14}$$

where $\mathbf{C}$ is a $K \times K$ matrix,

$$\mathbf{C} = \frac{1}{2\pi D} \sum_{d=1}^{D-1} \int_{-\pi}^{\pi} \phi(e^{j\omega/D} W_D^d) \phi^H(e^{j\omega/D} W_D^d) d\omega.$$

The problem becomes to minimize both the least square error $e_1(\mathbf{h})$ and the aliasing effect $\beta(\mathbf{h})$ with respect to some acceptable attenuation in the passband. A joint cost function can be formulated as

$$e_1(\mathbf{h}) + \beta(\mathbf{h}) = \mathbf{h}^T(\mathbf{A} + \mathbf{C})\mathbf{h} - 2\mathbf{h}^T \mathbf{b} + 1. \tag{15}$$

Combine this cost function with the min-max constraints (11), we have the following problem

$$\begin{cases} \min\limits_{\mathbf{h}} \mathbf{h}^T(\mathbf{A} + \mathbf{C})\mathbf{h} - 2\mathbf{h}^T \mathbf{b} + 1 \\ |H(e^{j\omega}) - H_d(e^{j\omega})| \leq \epsilon, \quad \forall \omega \in -[\omega_p, \omega_p] \end{cases} \tag{16}$$

where ϵ is the maximum deviation in the passband. This problem (16) can be solved using: (i) semi-infinite quadratic program technique or (ii) conventional quadratic programming using discretization. In this paper, we use the second method to design the prototype filter. The opitmazation problem is then reduced to a quadratic programming problem, which can then be solved using standard quadratic programming techniques.

4 Simulation Examples

In this section, performance comparison between the subband and the fullband approach is presented. This comparison is based on the MSE defined for all the sources,

$$\varepsilon_i = 10\log_{10}\left(\frac{\sum\limits_n |s_i[n] - u_i[n]|^2}{\sum\limits_n |s_i(n)|^2}\right), \quad 1 \leq i \leq 2, \quad (17)$$

where the summation is taken over the total number of transmitted symbols, which is set to 10^5 in all the simulations.

Comparison is also based on RFLOPS which is normalized to fullband (with one subband) FLOPS. The design of the prototype filter is excluded in the calculation of RFLOPS since this filter depends only on the number of subbands. The RFLOPS represents the computational complexity of the different equalization structures. The MSE and RFLOPS are evaluated and compared using a stochastic channel.

Example : Monte Carlo channel mixing matrix

A Monte Carlo simulation is run by using 30 random FIR channel mixing filters with length 10. The impulse responses for the mixing filters are generated from a gaussian distribution with mean 0 and variance 1. The ensemble average MSE are obtained by averaging the RFLOPS and the MSE.

Tables 1-2 compare the performance of the two prototype filters with 256–tap un-mixing filters at the receiver. The length of the prototype filters is four times the total number of subbands. The impulse response for the first prototype filter (Table 1) is obtained by minimizing the least square error criterion in conjunction with the Hamming window [9], while the impulse response for the second prototype filter (Table 2) is obtained by optimizing the filter performance and the in-band aliasing, see (16). Please note, that ϵ in (16) is chosen such that the filter has less than 1 dB attenuation in the passband. The MSE for the two sources is improved significantly by using the second prototype filter. This improvement is more distinct when the total number of subbands is large, e.g. $M = 16$ or $M = 32$.

The Tables also show the trade-off between the MSE and the RFLOPS when the number of subband increases from 4 to 32. The first row corresponds to the performance of the fullband solution ($M = 1$). When $M = 4$, the RFLOPS increases while the MSE remains approximately the same. This increased in computational complexity is due to the use of an over-sampled filterbank. Thus, M requires to be larger than four to have a computational reduction. When the number of subbands is increased to 8, the RFLOPS is reduced by 32% at an expense of 0.3 dB reduction in the MSE. The MSE are slightly lower with an increase in the number of subbands to $M = 16$ and $M = 32$.

5 Conclusions

In this paper, the performance of subband and fullband methods are compared for different number of subbands. Simulations have been performed for a stochastic channel. The results show that by properly optimizing the prototype filter, the subband performance is significantly improved. Moreover, the relative number of floating point operations is significantly reduced for more than four subbands at an expense of a small degradation in the MSE.

Future work includes further optimizing the prototype filter and incorporating adaptive estimation for the subband un-mixing filters. The adaptive estimation can be implemented by using a blind separation algorithm, e.g. independent component analysis (ICA) [3]. The advantage of a blind algorithm is that the training data (pilot sequence) is not required at the receiver.

6 Acknowledgement

The authors would like to thank Tech. Licentiate J. M. de Haan for uesfull discussion on filterbank design.

References

[1] G. Foschini, "Layered Space-Time Architecture for Wireless Communication in a Fading Environment when using Multi-element Antennas," Bell Labs Technical Journal, pp. 41-59, Autumn 1996.

[2] D. R. Morgan, and J. C. Thi, "A Delay-less Subband Adaptive Filter Architecture," *IEEE Trans. on Signal Processing*, vol. 43, no. 8, pp. 1819-1830, Aug 1995.

[3] N. Grbic, X. Tao, S. Nordholm, and Ingvar Claesson, "Blind Signal Separation Using Overcomplete Subband Representation," *IEEE Trans. on Speech and Audio Processing*, vol. 9, no. 5, July 2001.

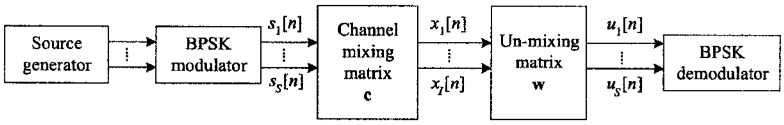

Figure 1: Channel model.

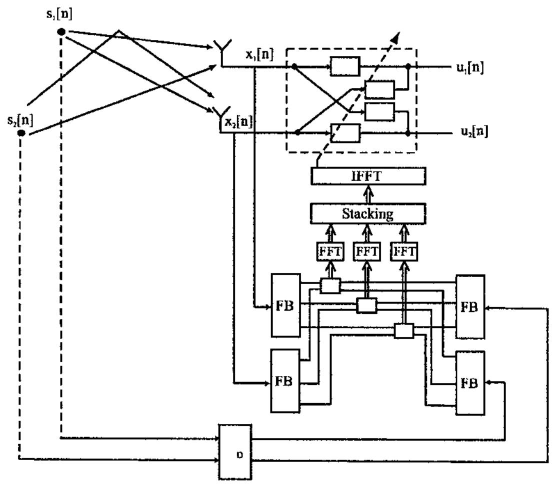

Figure 2: A non-causal delayed subband signal separation scheme.

[4] H. H. Dam, K. L. Teo, S. Nordebo, and A. Cantoni, "The Dual Parameterization Approach to Optimal Least Square FIR Filter Design Subject to Maximum Error Constraints," *IEEE Trans. Signal Processing*, vol. 48, pp. 2314–2320, no. 8, Aug. 2000.

[5] M. H. Hayes, *Statistical Digital Signal Processing and Modeling*, John Wiley & Sons, 1996.

[6] P. P. Vaidyanathan, *Multirate Systems and Filter Banks* Prentice Hall, 1993.

[7] T. W. Parks, C. S. Burrus, *Digital Filter Design* John Wiley & Sons Inc, 1987

[8] J. M. De Haan, N. Grbic, I. Claesson, and S. Nordholm, "Design of Oversampled Uniform DFT Filter Banks with Delay Specifications using Quadratic Optimization," *In Proc. The 2001 IEEE International Conference on Acoustics, Speech and Signal Processing*, ICASSP-01, vol. VI, pp. 3633–3636, Salt Lake City, USA, May 2001.

[9] Matlab: "Reference Guide," The Math Works, 1996.

Number	Prototype filter 1		
of subbands	RFLOPS	ε_1 [dB]	ε_2 [dB]
1	1.0	-28.4	-29.2
4	1.4	-28.0	-28.8
8	0.68	-27.5	-28.0
16	0.33	-25.9	-26.6
32	0.18	-22.6	-23.3

Table 1: Monte Carlo simulation with 256 taps for the un-mixing filters. Prototype filter 1 is obtained by minimizing the least square solution in conjunction with Hamming window method.

Number	Prototype filter 2		
of subbands	RFLOPS	ε_1 [dB]	ε_2 [dB]
1	1.0	-28.4	-29.2
4	1.4	-28.3	-29.0
8	0.68	-28.1	-28.8
16	0.33	-27.6	-28.4
32	0.18	-26.5	-27.1

Table 2: Monte Carlo simulation with 256 taps for the un-mixing filters. Prototype filter 2 is obtained by minimizing the filter performance in conjunction with the in-band aliasing effect.